Influence of stray fields on the switching-field distribution for bit-patterned media based on pre-patterned substrates

B. Pfau, C. M. Günther, E. Guehrs, Thomas Hauet, T. Hennen, S. Eisebitt, O. Hellwig

▶ **To cite this version:**

B. Pfau, C. M. Günther, E. Guehrs, Thomas Hauet, T. Hennen, et al.. Influence of stray fields on the switching-field distribution for bit-patterned media based on pre-patterned substrates. Applied Physics Letters, 2014, 105 (13), pp.132407. 10.1063/1.4896982 . hal-01282859

HAL Id: hal-01282859
https://hal.science/hal-01282859

Submitted on 13 Jul 2016

HAL is a multi-disciplinary open access archive for the deposit and dissemination of scientific research documents, whether they are published or not. The documents may come from teaching and research institutions in France or abroad, or from public or private research centers.

L'archive ouverte pluridisciplinaire **HAL**, est destinée au dépôt et à la diffusion de documents scientifiques de niveau recherche, publiés ou non, émanant des établissements d'enseignement et de recherche français ou étrangers, des laboratoires publics ou privés.

Influence of stray fields on the switching-field distribution for bit-patterned media based on pre-patterned substrates

B. Pfau,[1,a)] C. M. Günther,[2] E. Guehrs,[2] T. Hauet,[3,b)] T. Hennen,[3] S. Eisebitt,[1,2,4] and O. Hellwig[3]

[1]*Division of Synchrotron Radiation Research, Lund University, Box 118, 22100 Lund, Sweden*
[2]*TU Berlin, Institut für Optik und Atomare Physik, Hardenbergstraße 36, 10623 Berlin, Germany*
[3]*San Jose Research Center, HGST, A Western Digital Company, 3403 Yerba Buena Rd., San Jose, California 95135, USA*
[4]*Helmholtz-Zentrum Berlin für Materialien und Energie GmbH, Albert-Einstein-Str. 15, 12489 Berlin, Germany*

(Received 17 June 2014; accepted 20 September 2014; published online 1 October 2014)

Using a direct imaging method, we experimentally investigate the reversal of magnetic islands in a bit-patterned media sample based on a pre-patterned substrate. Due to systematic variation of the island distances in the media, we are able to study the influence of the dipolar interaction on the switching-field distribution of the island ensemble. The experimental findings are explained by an analytical magnetostatic model that allows us to quantify the different components of the demagnetizing field in the system and to distinguish intrinsic and dipolar broadening of the switching-field distribution. Besides the well-known dipolar broadening due to stray fields from neighboring islands, we find strong influence from the magnetized trench material on the island switching.
© 2014 Author(s). All article content, except where otherwise noted, is licensed under a Creative Commons Attribution 3.0 Unported License. [http://dx.doi.org/10.1063/1.4896982]

Reduction of switching-field distribution (SFD), i.e., island-to-island magnetic reversal-field variation is one of the major challenges in the development of bit-pattern media (BPM) data-storage technology.[1,2] Most of previous SFD studies focused on islands' intrinsic properties as these can possibly be improved in the growth process of the media. Island-to-island perpendicular-anisotropy variation, especially presence or absence of nucleation (trigger) crystalline grains with a lower-than-average anisotropy, has been found to be the main origin of intrinsic SFD.[3–5]

In the present work, we investigate the influence of the stray fields on the island reversal.[6–10] Even though long strings of identical up or down bits are usually forbidden to reduce demagnetization effects and ensure proper timing of bit read out, the design of BPM requires an effective understanding and meaningful modeling of these effects.[10–12] In this systematic experimental study, we keep track of the transition from an intrinsically governed SFD to a SFD dominated by stray fields. For this purpose, we have artificially enhanced the dipolar interactions in our model BPM system here by increasing the thickness and magnetization area density as compared to commonly used BPM systems[9,10,13–15] by about a factor of 6. We show that it is possible to precisely model such a system by magnetostatic considerations. Our analytical model particularly allows to understand the switching process for the extreme points at the onset of the reversal at low field (initialization field) and its saturation at high field (saturation field).

In order to distinguish between the intrinsic and dipolar SFD broadening, we have specifically designed a sample that contains four different patterned areas that were chosen to be identical except for the distance between the islands (pitch) as this parameter strongly influences the stray-field interaction, but not the islands' intrinsic properties. In this experimental setup, we can understand the impact of increasing dipolar interactions by directly comparing and modeling the magnetic field reversal of the four different patterned areas. To this end, we use a direct magnetic imaging method called x-ray Fourier-transform holography (FTH) that allows us to undisturbedly monitor the magnetic state of each island under an externally applied magnetic field.[16] Furthermore, the method is capable of imaging the four different patterned areas of interest independently at the same time, thus, ensuring exactly identical external conditions such as applied field and temperature.[17]

The sample was prepared by sputter deposition of a perpendicular anisotropy Co/Pd multilayer (Ta(15)/Pd(30)/$[Co(5.5)/Pd(8)]_{24}$/Pd(11) Å) onto a single pre-patterned Si_3N_4 membrane substrate containing all four patterned areas. Vibrating sample magnetometer measurements of the same continuous magnetic film prepared on a sister sample yielded a saturation magnetization of $M_s = (690 \pm 10)$ emu cm^{-3} normalized to the total multilayer thickness of 32.4 nm and a coercive field of (117 ± 5) Oe. The four patterned areas consist of periodic square arrays of cuboidal pillars with a lateral size of (80×80) nm^2 and a height of 40 nm. Due to that substrate topography, magnetic islands form on top of the pillars.[13,14] Material deposited in the trenches between the islands remains magnetically active, but is decoupled from the islands in terms of exchange interaction.

The patterned areas have an extent of (6×6) μm^2 each and are arranged in the corners of a square with 24 μm long

[a)]Author to whom correspondence should be addressed. Electronic mail: bastian.pfau@sljus.lu.se
[b)]Present address: Institut Jean Lamour, UMR CNRS 7198, Université de Lorraine, 54506 Vandoeuvre-lès-Nancy, France.

 © Author(s) 2014

This article is copyrighted as indicated in the article. Reuse of AIP content is subject to the terms at: http://scitation.aip.org/termsconditions. Downloaded to IP: 64.206.227.129 On: Thu, 02 Oct 2014 03:07:14

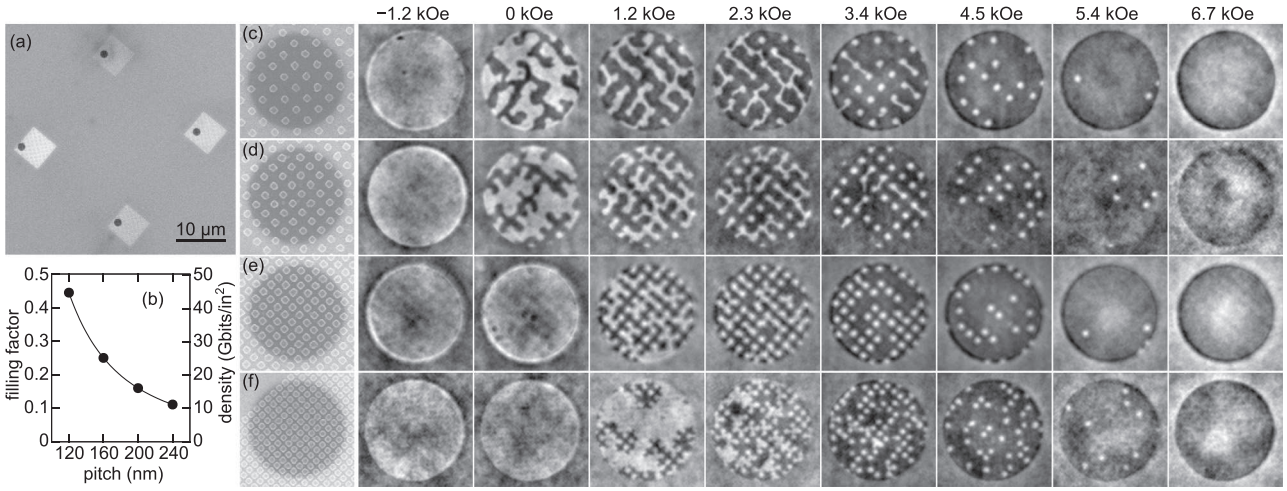

FIG. 1. (a) Arrangement of the patterned areas on the substrate (scanning electron microscope (SEM) image). (b) Conversion of the pitch length into the filling factor and storage density of the media. (c)–(f) Imaged magnetic reversal of the BPM with (c) 240 nm, (d) 200 nm, (e) 160 nm, and (f) 120 nm pattern pitch. First panel shows SEM image of each imaged area. Field steps are indicated on top. The FOV is 1.5 μm in diameter. The gray scale encodes out-of-plane magnetization with the magnetization direction pointing into the plane for bright areas and out of the plane for dark areas.

edges (Fig. 1(a)). The pattern pitch was varied from 120 nm up to 240 nm in steps of 40 nm. Each bit pattern was imaged in a constant field of view (FOV) with a diameter of 1.5 μm containing 29–112 islands depending on the pitch. Further details about the sample preparation and the imaging experiment can be found in our previous publication.[4]

In the experiments presented here, we imaged the system at different states in the magnetic hysteresis loop. In total, we have recorded 60 images for each FOV at 22 different field values within 10 hysteresis cycles always starting from saturation at −7.1 kOe. In Fig. 1, we present an example of the imaged reversal of the four magnetic systems. The image contrast purely encodes out-of-plane magnetization. The magnetic material remains saturated up to a field of approximately −1 kOe. At higher fields, the trench material starts to reverse its magnetization, so that the magnetic islands appear on the background of the already reversed trenches. The substrate pillars are strong pinning sites for the magnetic domain wall motion that dominates trench reversal. Consequentially, the pinning increases for the pattern with decreasing pitch corresponding to a higher density of pillars. The first islands switch their magnetization at an applied field between 1 kOe and 3 kOe again depending on the pitch. At a field of 6.7 kOe, the reversal is completed and the magnetization saturates in all patterned areas.

By counting the number of reversed islands (n) in each image acquired at a certain magnetic field (H), we are able to compile hysteresis loops of the island ensembles only,[10] i.e., to clearly decouple island and trench signals (Fig. 2). The normalized magnetization is determined by $M(H) = 2n(H)/N - 1$, where N represents the total number of islands visible in the FOV. The experimental data points are fitted with an asymmetric error function[9] which is analytically defined as an inverse function $H(M) = H_C + \sqrt{2}\sigma\,\mathrm{erf}^{-1}(M)/(1+\alpha M)$ where H_C denotes the coercive field, σ is the width (standard deviation) of the SFD, and α is the asymmetry parameter. The SFD is then numerically calculated as the probability distribution $\mathrm{d}M(H)/\mathrm{d}H$ of this fit.

The obvious changes in the hysteresis loops and, in particular, in the SFDs for an ever decreasing distance between the islands already demonstrate the strong influence of the magnetostatic interaction on the switching behavior. In Figs. 3(a)–3(c), we have plotted the hysteresis loop fit parameters as a function of the patterns' filling factor that is defined as the ratio of the area actually used for data storage (Fig. 1(b)). High filling factors, therefore, mean small pitch while low filling factors correspond to very sparse patterns. In the limit of the filling factor approaching zero, all interactions between the islands will vanish and one can directly extract the intrinsic properties of the islands.

In our experiments, the coercive field of the island ensemble slightly decreases with the filling factor while the width of the SFD strongly increases (Figs. 3(a) and 3(b)). These two effects result in a considerable increase of the SFD's full relative width ($2\sigma/H_C$) from 0.30 ± 0.02 (240 nm pitch) to 0.62 ± 0.02 (120 nm pitch).[9] In addition, the asymmetry also increases with the filling factor (Fig. 3(c)). The

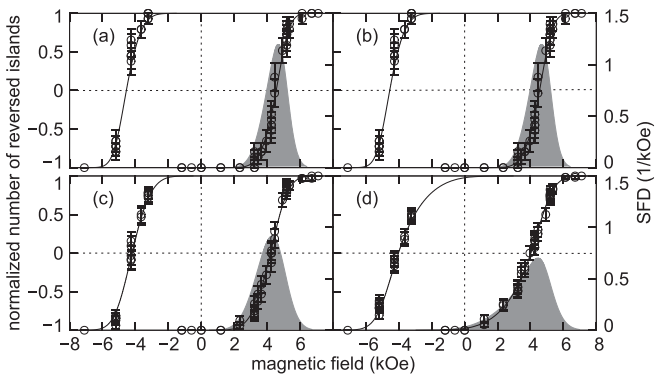

FIG. 2. Magnetic hysteresis loops of the island ensembles with (a) 240 nm, (b) 200 nm, (c) 160 nm, and (d) 120 nm pattern pitch extracted from the FTH images (examples shown in Fig. 1). The error bars of the experimental data points (open circles) account for the statistical error due to the limited ensemble size in the FOV.[4] The solid lines are fits to the experimental data points. The filled curves show the SFDs calculated from these fits.

This article is copyrighted as indicated in the article. Reuse of AIP content is subject to the terms at: http://scitation.aip.org/termsconditions. Downloaded to IP: 64.206.227.129 On: Thu, 02 Oct 2014 03:07:14

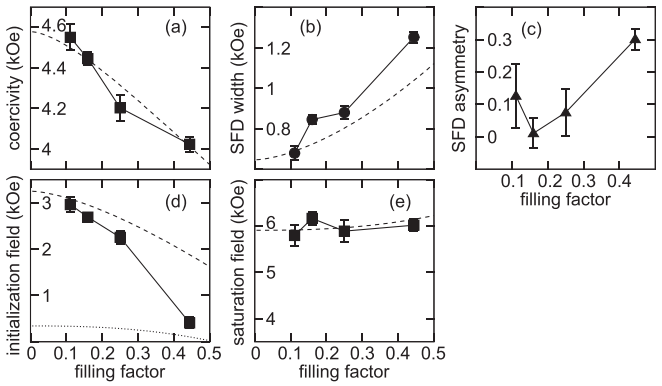

FIG. 3. Parameters resulting from fitting the hysteresis loops presented in Fig. 2: (a) coercive field (H_C), (b) width of the SFD (σ), and (c) asymmetry (α). (d) Initialization fields and (e) saturation fields as extracted from the same fits. The error bars were obtained from the uncertainty of the fits of the hysteresis loops. The dashed and dotted lines are calculations according to an analytical magnetostatic model as explained in the text.

initialization and the saturation field were extracted by thresholding the hysteresis fits to 2% switched islands and 2% remaining non-switched islands, respectively (Figs. 3(d) and 3(e)). The onset of the reversal shows a very strong dependence on the filling factor, while the saturation field is remarkably identical for all four patterned areas.

In order to explain the experimental observations, we calculated the demagnetization fields acting in the BPM system using a geometric magnetostatic model. The demagnetization field is decomposed into three contributions: (i) the internal demagnetization field of the island, (ii) the stray field from other islands, and (iii) the stray field from the trench material. We assess the shape of each island by a prism with a size defined by the design parameters, i.e., the lateral size of the pillars and the deposited height of the multilayer. In addition, we assume that the trenches between the islands are homogeneously filled by the multilayer material. The elevation distance between islands and trenches is given by the height of the substrate pillars. Our modeling does not take into account the deviation of the island shape from the perfect prism as observed by transmission electron micrographs of our BPM islands[4] and in other pre-pattern substrate-based BPM.[13,15] Furthermore, our assumption neglects any deposition shadowing effect in the trenches which becomes increasingly important at higher filling factors, i.e., when the ratio between the island height and the trench width becomes larger. If this ratio exceeds 1.5, shadowing effects can prevent any magnetic material in the trenches at all.[18] We will only discuss the out-of-plane component (z-component) of the fields, which corresponds to the material's easy anisotropy axis and to the direction of the applied field. Due to the symmetry of the arrangement, the in-plane components of the demagnetizing fields mostly vanish. It is further assumed that the non-reversed islands are magnetized as $M_i = -M_s$, and the trenches in the opposite direction ($M_t = M_s$).

The island's internal demagnetizing field (H_{intern}) can be calculated analytically as $-4\pi M_i N_{zz}$, where N_{zz} denotes the z-z-component of the demagnetizing tensor related to the prismatic shape.[19] The same relation is used to determine the stray field from the neighboring islands. In the distinguished case where all (identical) islands have the same magnetization direction, the resulting (maximum) demagnetization field (H_{island}) acting on an island is retrieved by numerically summing up the contributions from every island in the ensemble with regard to its relative distance. In a similar way, it is possible to calculate the demagnetization field of the saturated trenches (H_{trench}), as this field is composed out of the demagnetization field of the continuous film ($-4\pi M_t$) and the field generated by the prismatic magnetic voids that are created by the substrate pillars within the film. In the model, these voids have the same dimensions as the islands.

The demagnetization fields have different impact on the switching of an island. While the internal demagnetization field (Fig. 4(a)) promotes island switching[20] (it has positive sign), the already reversed film in the trenches (Fig. 4(c)) stabilizes the non-switched state (it has negative sign). At the beginning of the reversal process when most islands have not yet switched, the stray fields from the islands also promote island reversals, later, when most islands have switched, the resulting stray field stabilizes the last remaining non-reversed islands. This turnaround is the origin for the SFD broadening induced by dipolar interaction. Naturally, H_{intern} is equal for all islands as it only depends on the size and the shape of the islands. On the other hand, H_{island} and H_{trench} strongly depend on the filling factor. The stray field generated by the islands differs by nearly one order of magnitude (0.1 kOe to 0.8 kOe) for the sparsest and the densest arrangement considered here. In addition, it turns out that the stray field created by the trench material (−0.8 kOe to −1.2 kOe) is much stronger than the stray field from the surrounding islands.

In Figs. 4(d)–4(f), we show the calculated total demagnetization field for three prominent situations: (i) onset of the island switching ($H_{intern} + H_{island} + H_{trench}$), (ii) coercivity where on average the stray field from the islands vanishes ($H_{intern} + H_{trench}$), and (iii) saturation ($H_{intern} - H_{island} + H_{trench}$). In all three cases, it is assumed that the trench material completely reverses at lower fields than the islands. As will be discussed below, this assumption does not always hold for our sample, in particular in the case of high filling factors (cf. Fig. 1). Nevertheless, for much thinner BPM as usually used in high-density applications, this assumption is certainly

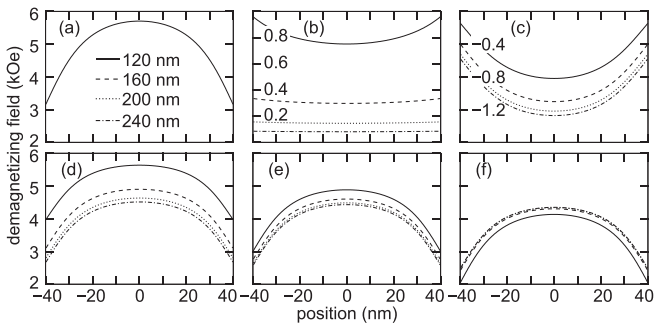

FIG. 4. Demagnetization fields (out-of-plane components) acting inside an island as obtained from analytical magnetostatic calculations for each of the four different patterned areas as indicated. The position axis corresponds to a slice through the center of the island parallel to an edge of the prismatic model island. First row shows the three demagnetization field contributions, (a) H_{intern}, (b) H_{island}, and (c) H_{trench}, as explained in the text. Second row depicts combinations of these fields for three prominent situations: (d) initialization of the switching, (e) coercivity, and (f) saturation.

This article is copyrighted as indicated in the article. Reuse of AIP content is subject to the terms at: http://scitation.aip.org/termsconditions. Downloaded to IP: 64.206.227.129 On: Thu, 02 Oct 2014 03:07:14

valid.[13,14] Remarkably, the *z*-component of the total demagnetization field always drastically decreases towards the edges of the islands by 1–2 kOe (Fig. 4(d)–4(f)).[7] We believe that this field loss is also responsible for the inactivity of trigger grains located in the periphery of the island as observed in Ref. 4.

Due to the systematic variation of the filling factor in our experiment, we are able to address the observed changes in the islands' switching field to the changes in the total demagnetization field acting on an island. This demagnetization field shifts the islands' effective switching field away from the intrinsic value. Consequentially, we use the above calculated total demagnetization fields to describe the dependence of the experimentally obtained initial (Fig. 3(d)), mean (Fig. 3(a)), and maximum (Fig. 3(e)) switching fields of the island ensembles on the filling factor. The islands' intrinsic switching fields serve as fit parameters. We have started with the fit of the ensembles' coercive fields (dashed line in Fig. 3(a)) where the mean intrinsic switching field (3.12 ± 0.03 kOe) is used as a parameter acting as a trivial field offset. The slope of the calculated curve—that is not fitted—matches the experimental findings. Consequentially, as predicted by the model, the decrease of the coercive field with increasing filling factor is solely caused by the influence of the trenches.

In a next step, we fit the experimentally obtained saturation fields using the calculated demagnetization fields for this scenario (dashed line in Fig. 3(e)). Again, this procedure includes an offset that in this case accounts for the intrinsic switching field of the magnetically hardest islands[4,5] of (4.45 ± 0.10) kOe corresponding to an increase of 1.3 kOe compared to the mean intrinsic switching field. The model reproduces that the saturation field is almost independent of the filling factor, which means that the changes in H_{island} and H_{trench} with the filling factor are in balance.

The experimentally observed strong decrease of the initialization field with the filling factor is only partly reproduced by the calculations. The dashed line in Fig. 3(d) is, therefore, obtained by using the same (negative) switching field deviation of the magnetically softest islands as for the hardest islands assuming a symmetric intrinsic SFD. This assumption reproduces the observation at low filling factors, where the intrinsic broadening dominates. The deviation at high density originates from the assumption of completely reversed trench material that becomes invalid at low fields (cf. Fig. 1). For the highest density, the first islands even switch under the influence of completely non-reversed trench material as indicated by the dotted line calculated from a total demagnetization field given by $H_{\mathrm{intern}} + H_{\mathrm{island}} - H_{\mathrm{trench}}$.

Using the previously calculated extreme points and neglecting the asymmetry, we have determined the standard deviation of a Gaussian SFD including intrinsic and additional dipolar broadening (Fig. 3(b)). In our model considering saturated trenches, the dipolar broadening is unaffected by the stray field of the trench material and, thus, only reflects the impact from the dipolar interaction between islands.[10–12] In the limit of very small filling factors, one obtains an estimate for the σ-width of the intrinsic SFD of 0.65 kOe. As can be presumed from the previous reasoning concerning the non-reversed trench material, the model reproduces the experimentally obtained width for low filling factors, but predicts lower values for high filling factors.

These findings lead to the conclusion that besides island–island interaction, part of the dipolar broadening of the SFD in our system and probably most of the asymmetry is caused by the strong influence of the trench material. The asymmetry mainly originates from the too-small difference of the coercive fields of the trench material and the island ensemble resulting in an asynchronous, but overlapping reversal of both parts. In an application context, the high magnitudes of the stray fields generated by the trench material would also result in an additional noise during readback.[2,15]

In order to suppress the influence from the trenches, different methods have been proposed to magnetically deactivate the trench material. During the sputtering process, one can exploit the above discussed shadowing effect, which can be even increased by first depositing an intermediate layer.[18] In another after-deposition approach, a suppression is reached by an additional annealing step triggering an interdiffusion of the trench material with the substrate.[15,21] Recently, most progress has been achieved by moving from pre-patterned substrates and subsequent blanket-deposition of the magnetic material to BPM based on full-film deposition with subsequent post-etching for forming isolated magnetic island BPM.[2,22,23] These systems completely avoid the noise and demagnetization challenges that trench material in BPM based on pre-patterned substrates presents.

In summary, we have systematically studied the island switching behavior in a BPM system with artificially enhanced dipolar interactions. By using a direct in-field imaging method, we were able to record hysteresis loops of the island ensembles and extract the SFD depending on the filling factor of the medium. We constructed a magnetostatic model that reproduces the experimental observations. Using this model, we have quantified the different demagnetization fields acting inside an island revealing the strong influence of the trench material. In addition, intrinsic properties of the islands were extracted. We conclude that our multi-object imaging method as well as the magnetostatic model considering basic geometrical shapes[20] provide valid tools in the design and research of BPM systems.

We thank H. Yang for help with fabrication of the pre-patterned membrane substrates.

[1]T. R. Albrecht, O. Hellwig, R. Ruiz, M. E. Schabes, B. D. Terris, and X. Z. Wu, *Nanoscale Magnetic Materials and Applications*, edited by J. P. Liu, E. E. Fullerton, O. Gutfleisch, and D. J. Sellmyer (Springer Science + Business Media, New York, 2009), pp. 237–274.
[2]O. Hellwig, L. J. Heydermann, O. Petracic, and H. Zabel, *Magnetic Nanostructures*, edited by H. Zabel and M. Farle (Springer, Berlin, Heidelberg, 2013) pp. 189–234.
[3]T. Thomson, G. Hu, and B. D. Terris, Phys. Rev. Lett. **96**, 257204 (2006).
[4]B. Pfau, C. M. Günther, E. Guehrs, T. Hauet, H. Yang, L. Vinh, X. Xu, D. Yaney, R. Rick, S. Eisebitt, and O. Hellwig, Appl. Phys. Lett. **99**, 062502 (2011).
[5]J. W. Lau, R. D. McMichael, S. H. Chung, J. O. Rantschler, V. Parekh, and D. Litvinov, Appl. Phys. Lett. **92**, 012506 (2008).
[6]T. Hauet, L. Piraux, S. K. Srivastava, V. A. Antohe, D. Lacour, M. Hehn, F. Montaigne, J. Schwenk, M. A. Marioni, H. J. Hug, O. Hovorka, A. Berger, S. Mangin, and F. Abreu Araujo, Phys. Rev. B **89**, 174421 (2014).
[7]K. Mitsuzuka, N. Kikuchi, T. Shimatsu, O. Kitakami, H. Aoi, H. Muraoka, and J. C. Lodder, IEEE Trans. Magn. **43**, 2160 (2007).

This article is copyrighted as indicated in the article. Reuse of AIP content is subject to the terms at: http://scitation.aip.org/termsconditions. Downloaded to IP: 64.206.227.129 On: Thu, 02 Oct 2014 03:07:14

[8]N. Thiyagarajah, H. Duan, D. L. Y. Song, M. Asbahi, S. H. Leong, J. K. W. Yang, and V. Ng, Appl. Phys. Lett. **101**, 152403 (2012).
[9]O. Hellwig, A. Berger, T. Thomson, E. Dobisz, Z. Z. Bandic, H. Yang, D. S. Kercher, and E. E. Fullerton, Appl. Phys. Lett. **90**, 162516 (2007).
[10]W. M. Li, Y. J. Chen, T. L. Huang, J. M. Xue, and J. Ding, J. Appl. Phys. **109**, 07B758 (2011).
[11]S. J. Greaves, Y. Kanai, and H. Muraoka, IEEE Trans. Magn. **44**, 3430 (2008).
[12]P. Krone, D. Makarov, T. Schrefl, and M. Albrecht, J. Appl. Phys. **106**, 103913 (2009).
[13]O. Hellwig, T. Hauet, T. Thomson, E. Dobisz, J. D. Risner-Jamtgaard, D. Yaney, B. D. Terris, and E. E. Fullerton, Appl. Phys. Lett. **95**, 232505 (2009).
[14]O. Hellwig, J. K. Bosworth, E. Dobisz, D. Kercher, T. Hauet, G. Zeltzer, J. D. Risner-Jamtgaard, D. Yaney, and R. Ruiz, Appl. Phys. Lett. **96**, 052511 (2010).
[15]O. Hellwig, A. Moser, E. Dobisz, Z. Z. Bandic, H. Yang, D. S. Kercher, J. D. Risner-Jamtgaard, D. Yaney, and E. E. Fullerton, Appl. Phys. Lett. **93**, 192501 (2008).
[16]S. Eisebitt, J. Lüning, W. F. Schlotter, M. Lörgen, O. Hellwig, W. Eberhardt, and J. G. Stöhr, Nature **432**, 885 (2004); O. Hellwig, S. Eisebitt, W. Eberhardt, J. Lüning, W. F. Schlotter, and J. Stöhr, J. Appl. Phys. **99**, 08H307 (2006).
[17]W. F. Schlotter, J. Lüning, R. Rick, K. Chen, A. Scherz, S. Eisebitt, C. M. Günther, W. Eberhardt, O. Hellwig, and J. Stöhr, Opt. Lett. **32**, 3110 (2007); B. Pfau, C. M. Günther, S. Schaffert, R. Mitzner, B. Siemer, S. Roling, H. Zacharias, O. Kutz, I. Rudolph, R. Treusch, and S. Eisebitt, New J. Phys. **12**, 095006 (2010).
[18]T. R. Albrecht and O. Hellwig, U.S. patent 8,130,468 B2 (6 March 2012).
[19]R. I. Joseph and E. Schlömann, J. Appl. Phys. **36**, 1579 (1965).
[20]J. Kalezhi, J. J. Miles, and B. D. Belle, IEEE Trans. Magn. **45**, 3531 (2009).
[21]E. E. Fullerton and O. Hellwig, U.S. patent 7,670,696 B2 (2 March 2010); E. E. Fullerton, O. Hellwig, J. S. Lille, J. T. Olson, P. A. van der Heijden, and H. H. Yang, U.S. patent 7,732,071 B2 (8 June 2010).
[22]T. R. Albrecht, D. Bedau, E. Dobisz, H. Gao, M. Grobis, O. Hellwig, D. Kercher, J. Lille, E. Marinero, K. Patel, R. Ruiz, M. E. Schabes, L. Wan, D. Weller, and T.-W. Wu, IEEE Trans. Magn. **49**, 773 (2013).
[23]O. Hellwig, E. E. Marinero, D. Kercher, T. Hennen, A. McCallum, E. Dobisz, T.-W. Wu, J. Lille, T. Hirano, R. Ruiz, M. K. Grobis, D. Weller, and T. R. Albrecht, J. Appl. Phys. **116**, 123913 (2014).

This article is copyrighted as indicated in the article. Reuse of AIP content is subject to the terms at: http://scitation.aip.org/termsconditions. Downloaded to IP: 64.206.227.129 On: Thu, 02 Oct 2014 03:07:14